

# Onset of a superconductor-insulator transition in an ultrathin NbN film under in-plane magnetic field studied by terahertz spectroscopy

M. Šindler <sup>\*</sup>, F. Kadlec , and C. Kadlec 

*Institute of Physics, Czech Academy of Sciences, Na Slovance 2, 182 21 Prague 8, Czech Republic*



(Received 31 August 2021; revised 8 November 2021; accepted 22 December 2021; published 6 January 2022)

Optical conductivity of a moderately disordered superconducting NbN film was investigated by terahertz time-domain spectroscopy in an external magnetic field applied along the film plane. The film thickness of  $\sim 5$  nm was comparable with the coherence length, so vortices should not form. This was confirmed by the fact that no marked difference between the spectra with a terahertz electric field set perpendicular and parallel to the external magnetic field was observed. Simultaneous use of Maxwell-Garnett effective medium theory and the model of optical conductivity by Herman and Hlubina [*Phys. Rev. B* **96**, 014509 (2017)] proved to correctly reproduce the terahertz spectra obtained experimentally in a magnetic field of up to 7 T. This let us conclude that the magnetic field tends to suppress the superconductivity, resulting in an inhomogeneous state where superconducting domains are enclosed within a normal-state matrix. The scattering rate due to pair-breaking effects was found to linearly increase with the magnetic field.

DOI: [10.1103/PhysRevB.105.014506](https://doi.org/10.1103/PhysRevB.105.014506)

## I. INTRODUCTION

In superconducting materials, the interactions between external static magnetic field and charge carriers are of fundamental importance. A magnetic field induces screening currents (orbital effect), and it interacts with the electron spin (Zeeman effect). Screening currents usually suppress the magnetic field in the bulk, so the Zeeman effect is weakened. However, an in-plane magnetic field will fully penetrate films whose thickness is much lower than the penetration depth  $\lambda$ ; therefore, the Zeeman effect can be dominant. In the case of low spin-orbit scattering, a magnetic field shifts the density of states (DOS) of electrons with spins up and down by  $\pm\mu_B\mu_0H$ , where  $H$  is the magnetic field intensity,  $\mu_0$  is the permeability of free space, and  $\mu_B = 9.274 \times 10^{-24}$  J T<sup>-1</sup> denotes the Bohr magneton. The spin-orbit scattering leads to spin flipping, and the spectroscopic gap  $\Omega_G$  is reduced by  $2\mu_B\mu_0H$ . As the spin-orbit scattering rate increases, peaks in the DOS due to up and down spins are smeared, and eventually, only one broad peak in the DOS remains. The spin-orbit scattering rate is proportional to the fourth power of the atomic number. Therefore, low spin-orbit scattering is typical of atoms with a low atomic number, which was confirmed by observations in Al films [1]. The field also breaks the time-reversal symmetry, causing an overall weakening of the superconducting state. Abrikosov and Gorkov [2] derived a theory describing superconductivity in the presence of magnetic impurities involving a pair-breaking parameter  $\alpha$ . Later, Maki [3] and de Gennes [4] proved that all ergodic pair-breaking perturbations contribute to the pair-breaking parameter  $\alpha$ . This applies also to ultrathin superconducting films—those having a thickness comparable with or smaller

than the coherence length—in the dirty limit, exposed to either in-plane or out-of-plane magnetic fields. These become effectively two-dimensional, and an in-plane magnetic field can induce a superconductor-insulator transition (SIT) [5,6]. The SIT introduces a nanoscale inhomogeneity, causing either an enhancement of coulombic interactions and a gradual decrease in the superconducting gap energy (fermionic scenario [7]) or a gradual loss of coherence within the condensate (bosonic scenario [8]). Such inhomogeneities were reported for various cases of the SIT [5,9,10].

To extend the knowledge of the behavior of ultrathin superconducting films, we studied the effects of an in-plane magnetic field on the optical conductivity by means of time-domain terahertz spectroscopy. We employed a custom-made experimental setup with an external magnetic field. Our measurements can provide access to the features which characterize the superconductivity, namely, the DOS, quasi-particle and Cooper-pair concentrations, vortex dynamics [11], and mesoscopic inhomogeneity. In this paper, we focus on the thinnest available NbN film from the series studied in Ref. [12] which shows an onset of the SIT.

## II. EXPERIMENT

The film was deposited on a  $10 \times 10 \times 1$  mm<sup>3</sup>-sized (100) MgO substrate by reactive magnetron sputtering of a 99.999% pure Nb target in a mixed Ar/N<sub>2</sub> atmosphere with partial pressures of  $P_{\text{Ar}} = 1.5 \times 10^{-3}$  mbar and  $P_{\text{N}_2} = 3.3 \times 10^{-4}$  mbar. The substrate holder was heated to 850 °C, and NbN was deposited at a rate of  $\sim 0.12$  nm/s. More details about the deposition technology can be found in Ref. [13]. The thickness of our film was determined from the known deposition rate as  $d = 5.3$  nm, which is close to the typical coherence length in NbN (4–7 nm [14]) and much less than the penetration depth  $\lambda = 2.3 \times 10^{-7}$  m, as estimated from the imaginary part

\*sindler@fzu.cz

of the complex conductivity at low frequencies. The critical temperature  $T_c = 13.9$  K was obtained in an independent DC resistivity measurement; this value is slightly lower than in the thicker samples from the same series (15.2 and 15.5 K for 14.5- and 30.1-nm-thick samples, respectively) [12]. We note that the critical temperature of NbN can reach up to 17.3 K [15].

Terahertz spectroscopy experiments consisted of measuring the sample transmittance using a custom-made time-domain spectrometer. Broadband terahertz pulses were generated using a Ti : sapphire femtosecond laser (Vitesse, Coherent) and a large-area interdigitated semiconductor emitter (TeraSED, GigaOptics). The sample was placed in an Oxford Instruments Spectromag He-bath cryostat with mylar windows and a superconducting coil, allowing for cooling the sample down to  $T = 2$  K. The Voigt geometry—i.e., an external static magnetic field directed along the sample plane—was used, and the magnetic field was varied up to the maximum value of  $\mu_0 H = 7$  T. The electric vector  $\mathbf{E}$  of the linearly polarized terahertz pulses was set either parallel or perpendicular to  $\mathbf{H}$ . The transmitted time profiles of electric field intensity  $E(t)$  were detected by phase-sensitive electro-optic sampling [16] in a 1-mm-thick (110) ZnTe crystal. The frequency ( $\nu$ ) dependence of complex transmittance  $\tilde{t}(\nu)$  was evaluated as the ratio between Fourier transforms  $E_s(\nu)$  and  $E_r(\nu)$  of the time profiles  $E(t)$  transmitted through the sample and a bare MgO reference substrate, respectively; this approach is known to effectively eliminate all instrumental functions. Before depositing the NbN film, we measured the time profiles of both the sample substrate and the reference including the Fabry-Perot reflections, from which we determined their thicknesses  $d_{\text{sub}}$  and  $d_r$ , respectively. More details and the error analysis can be found in Refs. [17,18]. For the purpose of the numerical computations of the complex conductivity of the film  $\tilde{\sigma}(\nu)$ , interference effects in the MgO substrates were avoided by truncating the measured time profiles before the echoes arising from internal reflections, whereas interferences in the thin film were accounted for [19]:

$$\tilde{t}(\nu) = \frac{E_s(\nu)}{E_r(\nu)} = \frac{[1 + \tilde{n}_{\text{sub}}(\nu)]e^{i\psi(\nu)}}{1 + \tilde{n}_{\text{sub}}(\nu) + Z_0\tilde{\sigma}(\nu)d}, \quad (1)$$

where  $Z_0$  denotes the vacuum impedance,  $\tilde{n}_{\text{sub}}(\nu)$  the complex refractive index of the substrate, and  $\psi(\nu)$  is the phase delay due to different optical thicknesses of the sample and reference. Since in both of these cases the same substrate material (MgO) was used, we can write

$$\psi(\nu) = \frac{2\pi\nu}{c} \{[\tilde{n}(\nu) - 1]d + \tilde{n}_{\text{sub}}(\nu)\Delta d\}, \quad (2)$$

where  $c$  is the light velocity, and  $\tilde{n}$  is the complex refractive index of the film. The first term in the curly brackets stems from the propagation in the film, and the second one reflects the difference in the thicknesses of the sample substrate and reference  $\Delta d = d_{\text{sub}} - d_r$ .

Alternatively, the complex conductivity of the film in the superconducting state  $\tilde{\sigma}^{\text{sc}}(\nu)$  can be obtained by assuming precise knowledge of the film conductivity  $\tilde{\sigma}^{\text{n}}(\nu)$  in the normal state just above  $T_c$ . In fact, as one evaluates the ratio of transmittances in the superconducting and normal states using

Eq. (1), the numerators cancel out, yielding

$$\frac{\tilde{t}_{\text{sc}}(\nu)}{\tilde{t}_{\text{n}}(\nu)} = \frac{1 + \tilde{n}_{\text{sub}}(\nu) + Z_0\tilde{\sigma}^{\text{n}}(\nu)d}{1 + \tilde{n}_{\text{sub}}(\nu) + Z_0\tilde{\sigma}^{\text{sc}}(\nu)d}, \quad (3)$$

from which  $\tilde{\sigma}^{\text{sc}}(\nu)$  can be evaluated. This simplification is possible because the optical properties of the MgO substrate change very weakly within such a narrow temperature interval. As an advantage, this approach is not affected by any inaccuracy in the value of  $\Delta d$ . The normal-state conductivity  $\tilde{\sigma}^{\text{n}}(\nu)$  was carefully determined previously [12].

### III. RESULTS AND DISCUSSION

In this paper, the sample was probed by linearly polarized terahertz pulses in two distinct geometries, with the electric-field vector  $\mathbf{E}$  parallel and perpendicular to the direction of the in-plane magnetic field, which we mark in the following by symbols  $E^{\parallel}$  and  $E^{\perp}$ , respectively. The complex conductivity of the film  $\tilde{\sigma}(\nu)$  was evaluated by the two above-described methods based on Eqs. (1) and (3).

#### A. Zero magnetic field

We start with the analysis of normal-state properties of our ultrathin NbN film. They were found to be accurately described by the Drude model, yielding a DC conductivity of  $\sigma_0 = (1.53 \pm 0.02) \mu\Omega^{-1}\text{m}^{-1}$  and a scattering time  $\tau_{\text{n}} = (15 \pm 8)$  fs [12]. The latter value indicates a moderate disorder, and in principle, quantum corrections to the Drude model might be applicable [20,21]. However, Cheng *et al.* [22] systematically studied NbN films with an increasing level of disorder, and quantum corrections appeared to play no significant role in their best-quality samples, exhibiting the highest values of  $T_c$ . Since the value of  $T_c$  in our film even slightly exceeds those reported in Ref. [22], we conclude that quantum corrections do not have to be considered.

In general, it is quite difficult to determine precisely the terahertz properties of superconducting films. This is especially true of the transmittance phase because one must distinguish between the contributions of the thin film and that of the substrate which is much thicker, in our case, by more than five orders of magnitude. We optimized the thickness difference  $\Delta d$  within the experimental accuracy so that terahertz spectra for  $H = 0$  show no dissipation [ $\sigma_1(\nu) \approx 0$ ] below the optical gap  $2\Delta$  in the zero-temperature limit. Indeed, this corresponds to the behavior expected for classical *s*-wave superconductors. By numerical calculations using Eq. (1), the precise mean value of the substrate thickness was found equal to the one determined previously  $d_{\text{sub}} = (990.0 \pm 0.5) \mu\text{m}$ . The alternative method of evaluating the NbN conductivity using Eq. (3) lead to the same results as those based on Eq. (1), see Fig. 1;  $\sigma_2(\nu)$  is shown in the Supplemental Material [23].

At zero magnetic field, the sample conductivity shows features typical of a classical Bardeen-Cooper-Schrieffer superconductor—below the optical gap  $2\Delta(0)$ , there is no dissipation in the real part, i.e.,  $\sigma_1 \approx 0$ , and a  $1/\nu$  dependence in the imaginary part  $\sigma_2(\nu)$  is observed (see black lines in Fig. 2). At low frequencies,  $\sigma_1 \ll \sigma_2$ ; thus,  $\sigma_1$  is determined less reliably than  $\sigma_2$ .

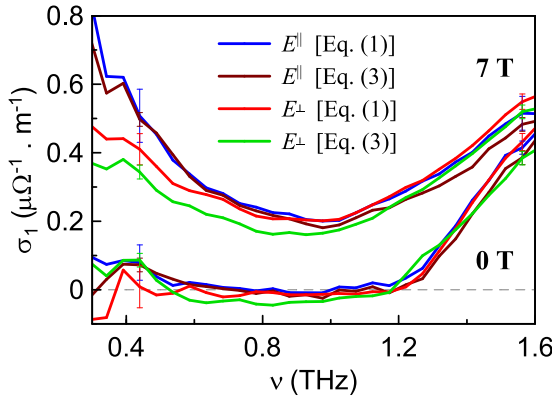


FIG. 1. Real part of spectra of NbN conductivity  $\sigma_1(\nu)$  obtained by the two described methods from experiments using both linear polarizations at  $T = 3$  K and a magnetic field of 0 and 7 T. Note that the evaluation of the imaginary part  $\sigma_2(\nu)$  provides spectra with a much lower uncertainty.

The zero-field conductivity can be best described by the Herman-Hlubina (HH) model for Dynes superconductors [24], see the red lines in Fig. 3. Within this model, the scattering rate in the normal state  $\Gamma_n$  can be written as a sum of two terms related to the superconducting state:  $\Gamma_n = \Gamma_s + \Gamma$ , where  $\Gamma_s$  and  $\Gamma$  are the scattering rates relative to the pair-conserving and pair-breaking processes, respectively. The parameter  $\Gamma$  also appears in the well-known Dynes formula [25], where it accounts for the broadening of the DOS which diverges at  $\pm\Delta$  for  $\Gamma = 0$ . The normal-state scattering rate is linked to the scattering time  $\tau_n$  by the relation  $\Gamma_n = (h/2\pi)(2\tau_n)^{-1}$ , where  $h$  is the Planck constant. In the

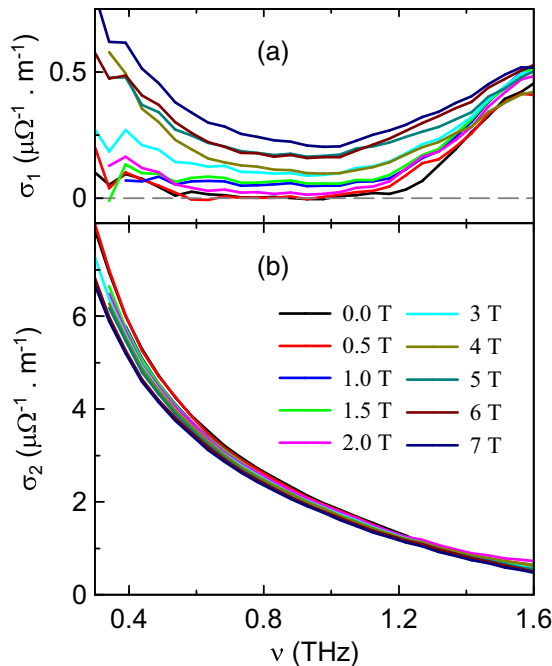


FIG. 2. (a) Real and (b) imaginary part of the conductivity of the NbN film under varying in-plane magnetic fields at  $T = 3$  K for  $E^{\parallel}$  evaluated using Eq. (1).

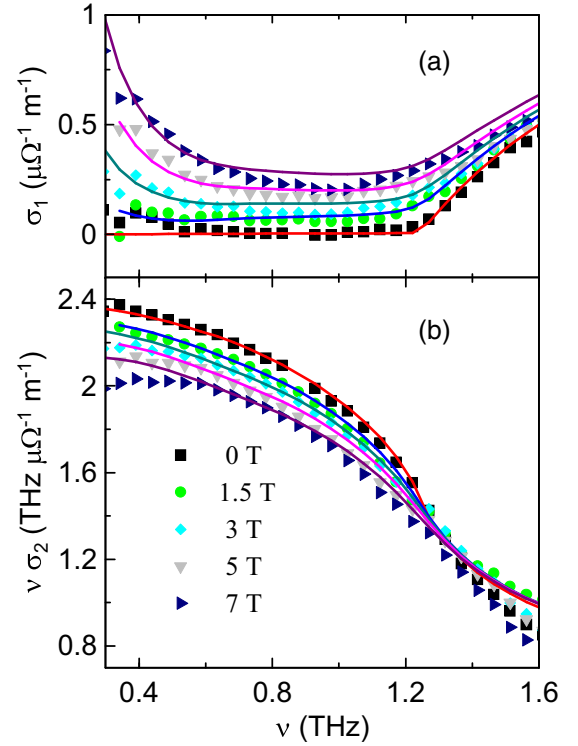


FIG. 3. Complex conductivity of NbN at  $T = 3$  K for  $E^{\parallel}$ , evaluated using Eq. (1). (a) Real part  $\sigma_1(\nu)$  and (b) imaginary part  $\nu\sigma_2(\nu)$ . Lines are fits by the Maxwell-Garnett formula [Eq. (4)] using the Drude model for the normal-state  $\tilde{\sigma}_n(\nu)$  and the Herman-Hlubina (HH) model for the superconducting-state  $\tilde{\sigma}_s(\nu)$  components, respectively.

limit  $\Gamma = 0$ , i.e., without pair-breaking processes, the HH model reproduces the Zimmermann model [26], which was successfully applied in the previous report on the ultrathin NbN sample [12]. In this paper, by fitting our zero-field spectra of the complex conductivity  $\tilde{\sigma}(\nu)$  using the HH model, we found  $\Gamma_s/h = (5.6 \pm 0.4)$  THz [27],  $\Gamma/h \leq 10^{-3}$  THz, and  $2\Delta(0)/h = 1.2$  THz. Due to the small value of  $\Gamma$ , the Zimmermann model is fully appropriate for the magnetic-field-free case. Indeed, from the values of scattering rates found in the superconducting state, we obtained  $\tau_n = (14 \pm 1)$  fs, which is in excellent agreement with the Drude fit of the normal-state spectra reported in Ref. [12]. However, unlike the HH model, the Zimmermann model is not able to account for modifications of the superconducting state due to magnetic field.

## B. Magnetic field dependence

Upon applying the in-plane magnetic field, the complex conductivity is modified, see Fig. 2. Whereas the imaginary-part spectra  $\sigma_2(\nu)$  vary only slightly even for the highest attainable field, the real-part spectra  $\sigma_1(\nu)$  show more significant changes. The dissipation increases with magnetic field; this occurs especially at low frequencies where an upward tail in  $\sigma_1(\nu)$  gradually develops. We did not observe any significant differences between the spectra corresponding to the terahertz pulses with linear polarizations parallel and perpendicular to the external magnetic field. By contrast, similar

experiments with a thicker NbN sample revealed a strongly polarization-dependent transmittance [28]. In the present case, the fact that the spectra for the two terahertz polarization directions are similar lets us conclude that the NbN sample contains no vortices oriented along the direction of the magnetic field, in contrast to predictions for thicker samples under an in-plane applied magnetic field [29]. This is in agreement with our estimate that the coherence length is comparable with the film thickness; thus, the vortex cores do not fit in.

Our experimental observations are different from those of Xi [14] and Xi *et al.* [30], who reported a prominent decrease in the gap energy upon increasing the magnetic field, whereas there was no dissipation below the gap. They successfully employed the model of complex conductivity developed by Skalski *et al.* [31]. Thus, we conclude that this model is not applicable in our case. The NbN sample studied by Xi *et al.* [32] was 70 nm thick; it had a critical temperature of  $T_c = 12.8$  K and a scattering time of  $\tau_n = 0.07$  fs, two orders of magnitude lower than in the present case. We suppose that the major difference in the spectral responses is linked to the sample thicknesses; whereas the sample in Ref. [30] was much thicker than the typical coherence length, the thickness of our sample was comparable with the coherence length. Consequently, only our sample can be considered as a two-dimensional system.

We assume that, upon applying an in-plane magnetic field, the superconducting properties are weakened by pair-breaking processes, and additionally, the system becomes inhomogeneous. In such a case, within the film, isolated superconducting islands are formed, surrounded by a matrix in which the superconducting properties are heavily suppressed; this part can be approximated by the normal state. The spectral response of superconducting islands is described by the HH model [24], where  $\Gamma$  plays a role analogous to the pair-breaking parameter  $\alpha$ . We have reproduced the experimental data by the Maxwell-Garnett model [33], in which the superconducting islands were treated as particles and the normal state as a matrix [12]:

$$\frac{\tilde{\sigma}_{\text{MG}}(\nu) - \tilde{\sigma}_n(\nu)}{L\tilde{\sigma}_{\text{MG}}(\nu) + (1-L)\tilde{\sigma}_n(\nu)} = f_s \frac{\tilde{\sigma}_s(\nu) - \tilde{\sigma}_n(\nu)}{L\tilde{\sigma}_s(\nu) + (1-L)\tilde{\sigma}_n(\nu)}, \quad (4)$$

where  $f_s$  and  $L$  are the volume fraction and the depolarization factor of the superconducting inclusions, respectively. Although the actual topology of the superconducting film can be nontrivial, we assume the depolarization factor to amount to  $L = \frac{1}{3}$ . This value is usually employed for calculating the response of flat disks embedded in a matrix, but it may equally describe other geometries.

The use of the Maxwell-Garnett formula for high concentrations of inclusions might be questioned. However, Rychetský *et al.* [34] argued that the Maxwell-Garnett formula holds even for high concentrations of inclusions if the matrix is percolated. In our fits, we used two fitting parameters: the volume fraction of superconducting islands  $f_s$  and the pair-breaking rate  $\Gamma$  which determines the shape of the  $\sigma_s(\nu)$  spectra. In fact, varying  $\Gamma_s$  and  $\Delta$  did not improve our fits, so we conclude that their values are independent of the magnetic field.

Our model describes correctly all observed spectral features, see Fig. 3. Terahertz conductivity spectra for both linear

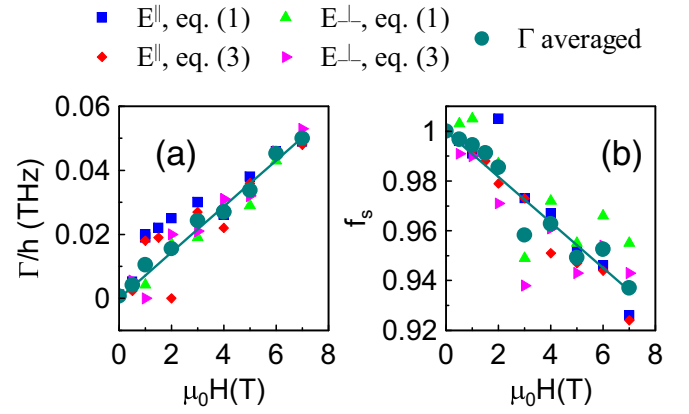


FIG. 4. (a) Cooper-pair-breaking scattering rate  $\Gamma$  and (b) volume fraction of superconducting inclusions  $f_s$  obtained from fits of  $\tilde{\sigma}(\nu)$  spectra at  $T = 3$  K as a function of applied in-plane magnetic field.  $\Gamma$  and  $f_s$  are the only two free parameters of the used Maxwell-Garnett model in combination with the Herman-Hlubina (HH) and Drude models. Lines: Fits demonstrating that both these parameters depend linearly on the magnetic field.

polarizations *evaluated by both methods* were fitted using only two free parameters:  $\Gamma$  and  $f_s$ , see Fig. 4. Although there is some scatter in the parameters, their field dependences exhibit clear trends. Whereas the volume fraction of superconducting inclusions  $f_s$  linearly decreases with  $H$  from 1 to 0.94, the pair-breaking scattering rate  $\Gamma$  linearly rises with the magnetic field as  $\Gamma/h = 0.0072$  THz T $^{-1} \mu_0 H$ , which corresponds to  $0.5 \mu_B \mu_0 H/h$ . The field dependences of  $f_s$  and  $\Gamma$  would be qualitatively the same if we assumed different values of  $L$ ; however, the experiment provides no means to obtain its most appropriate value.

The field dependences  $\Gamma(H)$  of the pair-breaking scattering rate upon a strong spin-orbit interaction were predicted to be quadratic for an in-plane magnetic field and linear for an out-of-plane field [35,36]. Xi *et al.* [30] performed far-infrared measurements under an in-plane magnetic field, and they evaluated the pair-breaking parameter  $\alpha$  using the Skalski model [31]. They obtained, in agreement with the theory, a quadratic dependence for a NbTiN thin film, but they also observed a linear behavior for their NbN film with  $\alpha/h = 0.014$  THz T $^{-1} \mu_0 H = \mu_B \mu_0 H/h$ . In contrast with our results, they observed no absorption below the optical gap, and they found a linear decrease in the spectroscopic gap  $\Omega_G$  with quite a steep slope of  $-0.12$  THz T $^{-1}$  ( $\sim 8.6 \mu_B/h$ ). This is different from the trend observed in our data which revealed only a small decrease in the optical gap even at the magnetic field of 7 T.

We believe that the observed linear dependence  $\Gamma(H)$  is due to a combination of Zeeman splitting of the DOS and the spin-orbit interaction. The peaks in the DOS become doublets due to the Zeeman effect, and they merge into a broad peak with a shape which can be well described by a formula pertinent for a Dynes superconductor. This assumption could be possibly verified by a direct observation of the DOS via tunneling measurements using an in-plane magnetic field. At a sufficiently strong field, a broad peak might transform into a doublet due to the increased strength of Zeeman splitting.



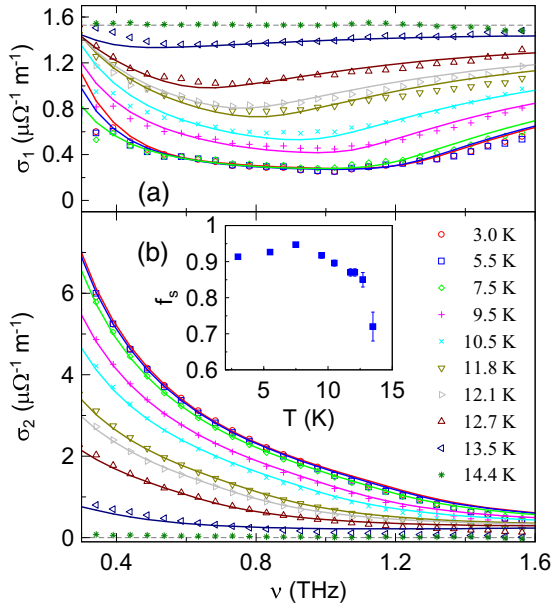


FIG. 5. (a) Real and (b) imaginary conductivity of NbN at  $\mu_0 H = 7$  T for linear polarization parallel with the external magnetic field evaluated from the transmission ratio  $t_{sc}/t_n$ . Lines: Fits using the Maxwell-Garnett [Eq. (4)], Herman-Hlubina (HH) (Ref. [24]), and Drude models. In the fitting, we used a temperature-dependent gap energy  $\Delta(T)$  expressed by Eq. (5), a temperature-independent scattering rate  $\Gamma$ , whereas the superconducting fraction  $f_s(T)$  was used as a free fitting parameter at each temperature. Inset: Temperature dependence of the superconducting fraction  $f_s$  obtained from the fits.

### C. Temperature dependence under magnetic field

To further test the validity of our model, we performed an additional set of measurements. It consisted in setting the magnetic field to the highest attainable value of  $\mu_0 H = 7$  T and measuring the temperature dependence of the conductivity of the NbN film. The experimental results (shown by symbols in Fig. 5) were evaluated from the transmission ratio  $\tilde{t}_{sc}/\tilde{t}_n$  [see Eq. (3)], where the normal-state transmittance was measured at  $T = 14.4$  K. In the fitting procedure, to account for the effect of heating, we approximated the temperature dependence of the gap by the expression [37]

$$\Delta(T) = \Delta(0) \sqrt{\cos \frac{\pi}{2} \left( \frac{T}{T_c} \right)^2}, \quad (5)$$

which for low values of  $\Gamma$ , yields results sufficiently close to the exact numerical calculations following the model of Herman and Hlubina [24]

The scattering rate  $\Gamma$  was assumed to be temperature independent, in agreement with previous measurements of different NbN samples [38]. In a MoC film, which is a similar superconducting compound,  $\Gamma$  was found to be temperature independent up to  $0.5 T_c$ , and at higher temperatures, it reached up to four times the low-temperature value [39]. Our model shows an excellent agreement with the experiment, see Fig. 5. This lets us conclude that, at fixed magnetic field of  $\mu_0 H = 7$  T, the superconducting fraction  $f_s$  is only weakly temperature dependent up to  $T = 10$  K, and it sharply decreases upon further heating (see inset of Fig. 5).

## IV. SUMMARY AND CONCLUSIONS

We studied the optical conductivity of a high-quality ultrathin NbN film under an in-plane applied external magnetic field of up to 7 T in the low-temperature limit. We measured its transmission in the terahertz range (0.4–1.6 THz), utilizing broadband pulses with linear polarization set either parallel or perpendicular to the applied static magnetic field, and we evaluated the complex conductivity spectra  $\tilde{\sigma}(\nu)$  using two different methods, one based on a direct computation [Eq. (1)] and one employing the ratio between the complex transmittances of the superconducting and normal states  $\tilde{t}_{sc}(\nu)/\tilde{t}_n(\nu)$  [Eq. (3)]. Both these approaches lead essentially to the same results, as shown in Fig. 1. Nevertheless,  $\tilde{\sigma}(\nu)$  can be determined more precisely by the latter method since the main source of experimental uncertainty originates in the thickness difference  $\Delta d$  which is effectively canceled in the ratio, and the relative errors in determining the conductivity values are lower in the normal state than in the superconducting one.

The zero magnetic field spectrum is well described by the Zimmermann model [26], as discussed in our previous publication [12]. In the present case, however, we used a more general model: that for Dynes superconductors proposed by Herman and Hlubina [24], which can consider the Cooper-pair-breaking processes. We found that the scattering rates in the normal and superconducting states are in excellent agreement ( $\Gamma_s = \Gamma_n$ ). The value of  $\Gamma$  is negligibly small, suggesting that Cooper-pair-breaking processes are weak, thus confirming the applicability of the Zimmermann model.

In the low-temperature limit, we observed a significant modification of the conductivity under an in-plane magnetic field. Its imaginary part is dominated by the London term  $\sigma_2(\nu) \sim 1/\nu$ , and it only slightly decreases with  $H$ . The real part  $\sigma_1(\nu)$  exhibits a marked absorption even at frequencies below the optical gap, which does not vanish even at the highest attained magnetic field. We did not observe any relevant difference between the spectra obtained in  $E^{\parallel}$  and  $E^{\perp}$  configurations, unlike in our previous experiments with thicker NbN films [28]. This absence of anisotropy rules out the presence of vortex chains predicted earlier by Luzhbin [29].

Our experimental results can be explained by assuming a local suppression of superconducting properties, resulting in an inhomogeneous state of superconducting islands in a normal-state matrix with a complex topology. The properties of superconducting islands are modified by pair-breaking effects proportional to the strength of the applied magnetic field. We found that, in the present case, the HH model for Dynes superconductors [24] is more suitable than the Skalski model [31]. An inhomogeneity on the nanoscale arising owing to the SIT was reported earlier in other cases [5,9,10]. To quantitatively describe our spectra, we developed a model assuming superconducting islands enclosed within a normal-state matrix based on the Maxwell-Garnett theory [33]. The complex topology was described by assuming a depolarization factor of  $L = \frac{1}{3}$ . Our model yields a linear decrease in the volume fraction of superconducting islands  $f_s$  with the magnetic field. At the same time, we observed a gradual decrease in the superconducting properties of our NbN film, which is reflected by the linear rise in the pair-breaking scattering rate  $\Gamma$  with the

magnetic field. Moreover, our approach has proved to remain valid also for higher temperatures.

Finally, we note that our experiment cannot provide a definite answer to whether the SIT occurs via the bosonic or fermionic scenario because we observed only the onset of the transition, even at the highest attainable magnetic field. However, the decrease in the volume fraction of the superconducting inclusions  $f_s$  and the constant value of the optical gap with increasing magnetic field slightly favor the bosonic scenario.

## ACKNOWLEDGMENTS

We are grateful to K. Ilin and M. Siegel for preparing and characterizing the NbN sample as well as to F. Herman and R. Hlubina for fruitful discussions. We also acknowledge the financial support by the Czech Science Foundation (Project No. 21-11089S) and by the Operational Programme “Research, Development and Education” financed by European Structural and Investment Funds and the Czech Ministry of Education, Youth and Sports (Project No. SOLID21-CZ.02.1.01/0.0/0.0/16\_019/0000760).

- 
- [1] R. Meservey, P. M. Tedrow, and P. Fulde, *Phys. Rev. Lett.* **25**, 1270 (1970).
- [2] A. A. Abrikosov and L. P. Gor'kov, *Zh. Eksp. Teor. Fiz.* **39**, 1781 (1961) [*Sov. Phys. JETP* **12**, 1243 (1961)].
- [3] K. Maki, in *Superconductivity*, edited by R. D. Parks (Marcel Dekker, Inc., New York, 1969), Vol. 2, Chap. 18, p. 1035.
- [4] P. G. de Gennes, *Phys. Kondens. Mater.* **3**, 79 (1964).
- [5] V. F. Gantmakher, M. V. Golubkov, V. T. Dolgoplov, A. Shashkin, and G. E. Tsydynzhapov, *J. Exp. Theor. Phys. Lett.* **71**, 473 (2000).
- [6] K. A. Parendo, K. H. S. B. Tan, and A. M. Goldman, *Phys. Rev. B* **73**, 174527 (2006).
- [7] A. M. Finkel'stein, *Pisma Zh. Eksp. Teor. Fiz.* **45**, 37 (1987) [*Sov. JETP Lett.* **45**, 46 (1987)].
- [8] M. P. A. Fisher, P. B. Weichman, G. Grinstein, and D. S. Fisher, *Phys. Rev. B* **40**, 546 (1989).
- [9] B. Sacépé, C. Chapelier, T. I. Baturina, V. M. Vinokur, M. R. Baklanov, and M. Sanquer, *Phys. Rev. Lett.* **101**, 157006 (2008).
- [10] Y. Noat, V. Cherkez, C. Brun, T. Cren, C. Carillet, F. Debontridder, K. Ilin, M. Siegel, A. Semenov, H.-W. Hübers, and D. Roditchev, *Phys. Rev. B* **88**, 014503 (2013).
- [11] M. Dressel, *Adv. Condens. Matter Phys.* **2013**, 104379 (2013).
- [12] M. Šindler, C. Kadlec, P. Kužel, K. Ilin, M. Siegel, and H. Němec, *Phys. Rev. B* **97**, 054507 (2018).
- [13] D. Henrich, S. Dörner, M. Hofherr, K. Il'in, A. Semenov, E. Heintze, M. Scheffler, M. Dressel, and M. Siegel, *J. Appl. Phys.* **112**, 074511 (2012).
- [14] X. Xi, Conventional and time-resolved spectroscopy of magnetic properties of superconducting thin films, dissertation thesis, University of Florida, 2011.
- [15] C. P. Poole, Jr., H. A. Farach, R. J. Creswick, and R. Prozorov, *Superconductivity* (Academic Press, Amsterdam, 2007).
- [16] A. Nahata, J. T. Yardley, and T. F. Heinz, *Appl. Phys. Lett.* **75**, 2524 (1999).
- [17] C. Kadlec, F. Kadlec, H. Němec, P. Kužel, J. Schubert, and G. Panaitov, *J. Phys.: Condens. Matter* **21**, 115902 (2009).
- [18] F. Kadlec, C. Kadlec, P. Kužel, and J. Petzelt, *Phys. Rev. B* **84**, 205209 (2011).
- [19] We are using the convention  $E(t) = E_0 \exp(-i\omega t)$ , which implies the following forms of the complex quantities: conductivity  $\tilde{\sigma} = \sigma_1 + i\sigma_2$ , permittivity  $\tilde{\epsilon} = \epsilon_1 + i\epsilon_2$ , and refractive index  $\tilde{n} = n + ik$ .
- [20] B. L. Alsthuler and A. G. Aronov, in *Electron-Electron Interactions in Disordered Systems*, edited by V. M. Agranovich and A. A. Maradudin (North-Holland, Amsterdam, 1987).
- [21] P. Neilinger, J. Greguš, D. Manca, B. Grančič, M. Kopčík, P. Szabó, P. Samuely, R. Hlubina, and M. Grajcar, *Phys. Rev. B* **100**, 241106(R) (2019).
- [22] B. Cheng, L. Wu, N. J. Laurita, H. Singh, M. Chand, P. Raychaudhuri, and N. P. Armitage, *Phys. Rev. B* **93**, 180511(R) (2016).
- [23] See Supplemental Material at <http://link.aps.org/supplemental/10.1103/PhysRevB.105.014506> for further figures displaying all our experimental data and fits.
- [24] F. Herman and R. Hlubina, *Phys. Rev. B* **96**, 014509 (2017).
- [25] R. C. Dynes, V. Narayanamurti, and J. P. Garno, *Phys. Rev. Lett.* **41**, 1509 (1978).
- [26] W. Zimmermann, E. Brandt, M. Bauer, E. Seider, and L. Genzel, *Physica C* **183**, 99 (1991).
- [27] Throughout this paper, we express energy in terahertz units, as it allows for a direct comparison with experimental spectra  $\sigma(\nu)$ . The energy can be calculated by multiplying by the Planck constant  $h$ . The scattering time  $\tau$  is related to the energy scale  $E$  by  $E = \hbar/\tau$ , where  $\hbar$  is the reduced Planck constant.
- [28] M. Šindler, R. Tesař, J. Koláček, and L. Skrbek, *Physica C* **533**, 154 (2017).
- [29] D. A. Luzhbin, *Phys. Solid State* **43**, 1823 (2001).
- [30] X. Xi, J. Hwang, C. Martin, D. B. Tanner, and G. L. Carr, *Phys. Rev. Lett.* **105**, 257006 (2010).
- [31] S. Skalski, O. Betbeder-Matibet, and P. R. Weiss, *Phys. Rev.* **136**, A1500 (1964).
- [32] X. Xi, J.-H. Park, D. Graf, G. L. Carr, and D. B. Tanner, *Phys. Rev. B* **87**, 184503 (2013).
- [33] J. C. M. Garnett and J. Larmor, *Philos. Trans. R. Soc. London A* **203**, 385 (1904).
- [34] I. Rychetský, M. Glogarová, and V. Novotná, *Ferroelectrics* **300**, 135 (2004).
- [35] M. Tinkham, *Introduction to Superconductivity* (McGraw-Hill, New York, 1996).
- [36] P. Fulde, *Mod. Phys. Lett. B* **24**, 2601 (2010).
- [37] T. P. Sheahan, *Phys. Rev.* **149**, 368 (1966).
- [38] M. Šindler, R. Tesař, J. Koláček, P. Szabó, P. Samuely, V. Hašková, C. Kadlec, F. Kadlec, and P. Kužel, *Supercond. Sci. Technol.* **27**, 055009 (2014).
- [39] P. Szabó, T. Samuely, V. Hašková, J. Kačmarčík, M. Žemlička, M. Grajcar, J. G. Rodrigo, and P. Samuely, *Phys. Rev. B* **93**, 014505 (2016).